Surface Science 108 (1981) 368–380
North-Holland Publishing Company

INTERACTION OF C_2N_2 WITH CLEAN AND OXYGEN DOSED Cu(111) SURFACE STUDIED BY AES, ELS AND TDS MEASUREMENTS

F. SOLYMOSI and J. KISS

Reaction Kinetics Research Group, The University, P.O. Box 105, H-6701 Szeged, Hungary

Received 14 January 1981; accepted for publication 2 March 1981

The adsorption and surface reaction of cyanogen on clean and oxygen covered Cu(111) have been investigated. From electron energy loss measurements, thermal desorption spectroscopy and electron beam effects in Auger spectroscopy, it is proposed that cyanogen adsorbs dissociatively on Cu(111) at 300 K. The activation energy for the desorption was calculated to be 180 kJ/mol. Cyanogen adsorption onto oxygen predosed Cu(111) is inferred to produce the NCO surface species. This interpretation was aided by data of electron energy loss measurements and from HNCO adsorption onto Cu(111) at 300 K. A reaction began in the co-adsorbed layer above 400 K, yielding CO_2 and N_2.

1. Introduction

We recently investigated the interaction of isocyanic acid, HNCO, with a Cu(111) surface [1,2]. No detectable adsorption was observed on a clean surface at 300 K. The presence of adsorbed oxygen, however, greatly promoted the interaction between the HNCO and the copper surface and caused the dissociative adsorption of the HNCO.

The surface NCO was found to be stable up to 400 K, but above this temperature it reacted with chemisorbed oxygen. The products of the reaction were CO_2 (T_{max} = 463 and 633 K) and N_2 (T_{max} = 793 K). Above 800 K, after consumption of adsorbed oxygen, the formation of cyanogen (C_2N_2) was observed.

As the interaction of C_2N_2 with Cu surfaces has not yet been investigated, a detailed study of the adsorption and desorption of C_2N_2 on and from this surface promised useful data relating to the mechanisms of NCO decomposition and of C_2N_2 formation.

The adsorption of C_2N_2 has previously been studied by LEED, Auger spectroscopy and thermal desorption mass spectrometry on Pt(100), Pt(110), Ag(110) and Ni(111) surfaces [3–11]. On both Pt surfaces three adsorption states (α, β_1 and β_2) were observed. The more weakly bound α state was thought to consist of molecularly (i.e. non-dissociatively) adsorbed C_2N_2 [3–6]. There is some controversy, however, as regards the β states. Lambert et al. [6] state that the β phases are due to

0039-6028/81/0000–0000/$02.50

the associative desorption of pairs of CN radicals formed in the surface dissociation of C_2N_2. The occurrence of the dissociative adsorption of C_2N_2 was claimed to be confirmed by the results of HCN adsorption studies [12], where both $CN_{(a)}$ and $C_2N_{2(a)}$ desorb exclusively as C_2N_2. In contrast, taking into account electron energy loss and UPS measurements, Netzer et al. [4,7,8] argue against the dissociated adsorption model and suggest the formation of two-dimensional paracyanogen-like units. In support of this assumption they mention the marked contrast between the ELS of Pt(100)/CO and Pt(100)/C_2N_2 in the lower energy loss region, and direct identification of the C–C bond by UPS measurements [7,8].

On an Ag(110) surface, the adsorption–desorption of C_2N_2 is reversible and involves associatively adsorbed C_2N_2 [5]. The presence of adsorbed rubidium, however, induces dissociation of cyanogen during chemisorption and leads to a mixed adlayer containing two kinds of surface cyanide species [11].

C_2N_2 on the Ni(111) surface forms an extremely stable, ordered (6 × 6) structure [10], decomposition of which at ~800 K leads to complete removal of nitrogen as N_2.

2. Experimental

Experiments were performed in a stainless steel UHV chamber described in detail elsewhere [2]. The chamber was equipped with a 3-grid retarding field analyzer for low-energy electron diffraction (LEED), and a single-pass CMA analyzer for Auger analysis and for electron energy loss measurements, with a quadrupole mass analyzer to monitor gas-phase composition and with several gas inlets. The vacuum system was evacuated with ion pumps and a titanium getter. A base pressure of 1.5×10^{-10} Torr was reached.

The oriented disk-shaped crystal (diameter 6 mm, thickness 1.5 mm) was obtained from Metals Research Corporation. The sample was heated from the rear by the radiation of a tungsten filament. The temperature was measured with a chromel–alumel thermocouple spot-welded to the edge of the crystal. The surface was cleaned by cycles of Ar^+ bombardment and annealing at 973 K for some min.

C_2N_2 was prepared by thermal decomposition of AgCN in a glass cell attached to the UHV system, and was directed towards the crystal surface by a capillary [4].

3. Results

3.1. Clean surface

We first investigated the adsorption of C_2N_2 on a clean Cu(111) surface. Exposure of the Cu(111) surface to C_2N_2 at 300 K resulted in the appearance of N and C KLL signals at 384 and 271 eV (fig. 1). However, it produced no additional diffrac-

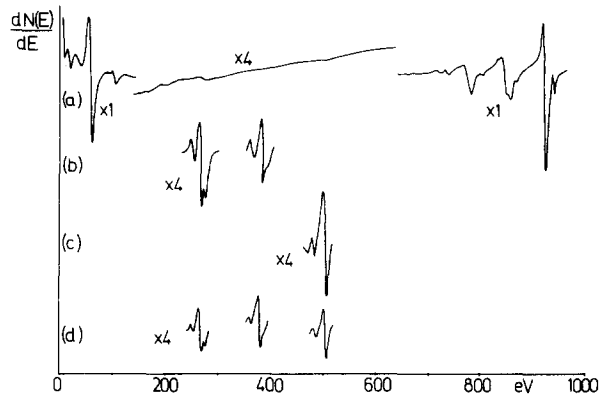

Fig. 1. Auger spectra of the Cu(111) surface taken at 300 K: (a) with clean surface; (b) after exposure to 9 L C_2N_2; (c) after exposure to 60 L O_2; (d) after exposure of the oxygen covered surface ($\theta \sim 0.17$) to 90 L C_2N_2.

tion spots in the LEED pattern of the clean Cu(111) surface. An increase of the diffuse background was observed. In fig. 2 the ratios of N and C signals to the Cu 920 eV signal are shown. Saturation values were reached at about 20 L C_2N_2. Taking into account the relative sensitivity of Auger electron spectroscopy as regards carbon and nitrogen (~1.5), we obtain approximately a value of 0.85 for the carbon/nitrogen ratio. The initial sticking probability is about 0.1. It was estimated from plots of relative N Auger signal as a function of total exposure. As the results plotted in fig. 3A indicate, the electron beam exerted a negligible effect on the intensities of the N and C signals.

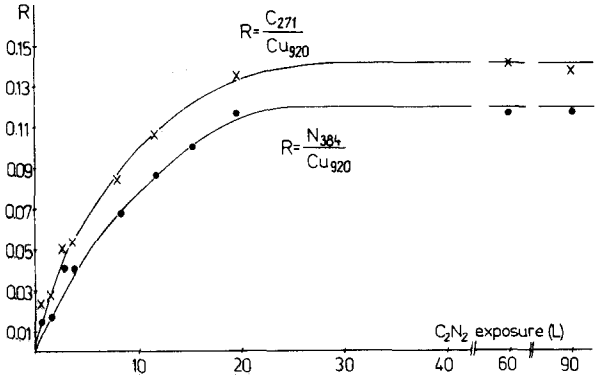

Fig. 2. The dependence of the relative C and N signals on the C_2N_2 exposure at 300 K.

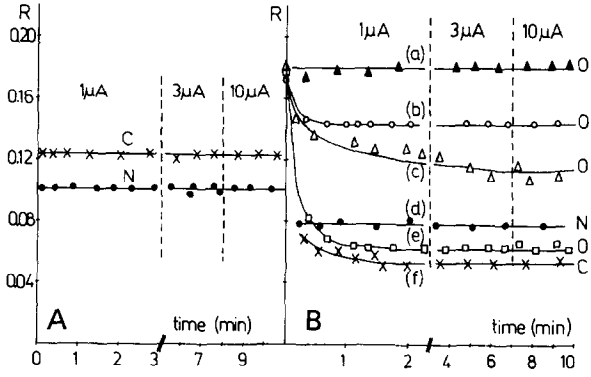

Fig. 3. The effect of the beam current and beam exposition on the relative intensities of N, C and O Auger signals. (A) Clean surface exposed to 90 L C_2N_2. (B) Oxygen covered surface ($\theta \sim 0.17$) at different C_2N_2 exposures. (a) 0 L C_2N_2, (b) 18 L C_2N_2, (c) 60 L C_2N_2, (d–f) 90 L C_2N_2. ($R = C_{271}/Cu_{920}; N_{384}/Cu_{920}; O_{514}/Cu_{920}$).

The thermal desorption spectra of C_2N_2 (amu 52) are shown in fig. 4. In harmony with the results of Auger studies, saturation was reached at approximately 25 L. Desorption of C_2N_2 began above 700 K. In a search for other adsorption stages, the exposure of C_2N_2 was increased far above the value required for saturation. On exposure to 90 and 180 L a very small amount of C_2N_2 was detected at 300–400 K. The area of this peak was only about 6% of that of the main peak. No nitrogen (14 and 28 amu) was identified in the desorbing gases. During the desorption a little CN (26 amu) was also detected, its amount corresponding to that formed in the fragmentation of C_2N_2 due to electron impact.

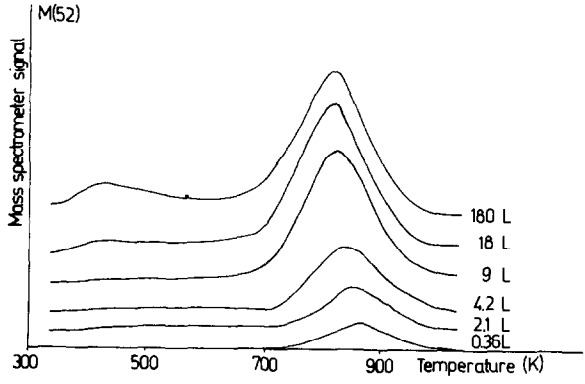

Fig. 4. Thermal desorption spectra following C_2N_2 adsorption on Cu(111) surface at 300 K.

Table 1
Some characteristic data for the adsorption and desorption of C_2N_2 on and from metal surfaces

Sample	Ref.	LEED	Coverage (molecules/cm^2)	Sticking coefficient		Thermal desorption					
						α		β_1		β_2	
				α	β	T_{max} (K)	E [a]	T_{max} (K)	E	T_{max} (K)	E
Pt(100)	[3,4]	(5 × 1) → (1 × 1) Disordered	$\theta \approx 0.5$ 2×10^{14}, 5.5×10^{14}	0.06	0.9	413	50.2	683	133	753	175.8
Pt(110)	[6]	(1 × 2) → (1 × 1) Disordered				460	119	>673		<873	210
Pt(111) Stepped	[9]	Disordered	7×10^{14}			405		690		780	
Ag(110)	[5]	Disordered				430					
Ni(111)	[10]	(6 × 6) at 400 K						800 (N_2)			
Cu(111) clean	This work		$\theta \approx 0.2$ $3.6 \pm 1 \times 10^{14}$	~0.1				870–815	180 (C_2N_2)		
Cu(111) oxygen dosed	This work		Decreasing with oxygen coverage					820	160 (C_2N_2) [b]		
								490	57 ($CO_2\alpha_1$)		
								613	99 ($CO_2\alpha_1$)		
								690	– ($CO_2\alpha_3$)		
								810	146 (N_2)		

[a] E, activation energy for desorption, in kJ mol^{-1}
[b] Oxygen coverage, θ, was ~0.02.

The peak temperature of C_2N_2 desorption decreased slightly with the increase of coverage from 870 K to 815 K, apparently indicating a second-order process. Quantitative analysis of the area under the pressure curve yielded a saturation value of $(3.6 \pm 1) \times 10^{14}$ molecules/cm^2. The activation energy for the desorption was calculated on base of heating rate variation method. The resulting values are shown in table 1.

3.2. Oxyen-dosed surface

In contrast to the adsorption of HNCO, preadsorbed O_2 on a Cu(111) surface resulted in no promoted adsorption of C_2N_2. With increase of the oxygen coverage, the extent of C_2N_2 adsorption gradually decreased. Fig. 5 shows the effect of the oxygen coverage on the relative Auger signals of N and C. The C_2N_2 exposure was 90 L.

It was interesting that on the clean Cu(111) surface, and also on the surface containing only a small amount of oxygen ($O_{514}/Cu_{920} = 0.024$, corresponding to about 0.02 coverage), the C_{271}/Cu_{920} value always exceeded that of N_{384}/Cu_{920}, whereas at higher oxygen coverage the situation was the reverse.

Another feature worth mentioning is that a much lower O signal was measured after adsorption of C_2N_2 than before (fig. 3B). A plausible explanation for this

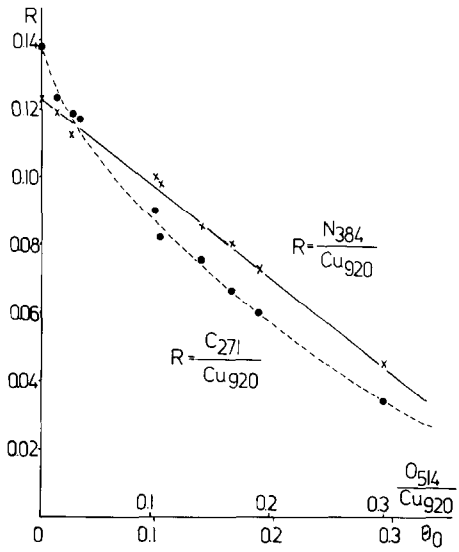

Fig. 5. The effect of oxygen coverage on the relative Auger signals of N and C. The exposition of C_2N_2 was 90 L. The absolute coverage of oxygen was calculated similarly as in our previous work [2] by using the relationship found by Bootsma et al. [13] between the ratio h_O/h_{Cu} in the Auger spectra and $\delta\Delta$ (ellipsometry) as well as between $\delta\Delta$ and the oxygen coverage.

phenomenon is that the C_2N_2 replaced some of the adsorbed oxygen, or reacted with chemisorbed oxygen. We could not detect any gaseous products during the adsorption of C_2N_2 at 300 K however, not even when the analyzer of the mass spectrometer was in front of the sample (~20 mm). No reaction products were found when the C_2N_2 was admitted at 373 K. Nevertheless, we observed that, whereas there was only a very slight decrease in the oxygen signal with the increase in the duration of the beam exposure and the beam current before the adsorption of C_2N_2, after the adsorption the oxygen signal became very sensitive to the electron beam (fig. 3B). The extent of the decrease in the intensity of O signal depended on the C_2N_2 exposure.

In contrast to the results obtained on the clean surface with increasing exposure to the electron beam a slight decrease was experienced in the relative intensity of the C signal. No change was observed in the N signal, even at high beam current (fig. 3B).

The thermal stability of adsorbed C_2N_2 was investigated at two different O_2 coverages. When the sample was heated after the adsorption of C_2N_2 on an oxygen-dosed surface (coverage ~0.02), CO_2 evolution was first detected. The CO_2 desorbed in three stages, the characteristic temperatures of these stages being 490, 613 and 690 K. The peak maximum of the desorption of C_2N_2 was 820 K. Nitrogen desorbed above 750 K, with a peak maximum of 810 K. No CO or nitrogen oxide was detected in the desorbing gases. Calculations based on the determination of the desorbed products showed that about 13% of the adsorbed C_2N_2 had been oxidized to CO_2.

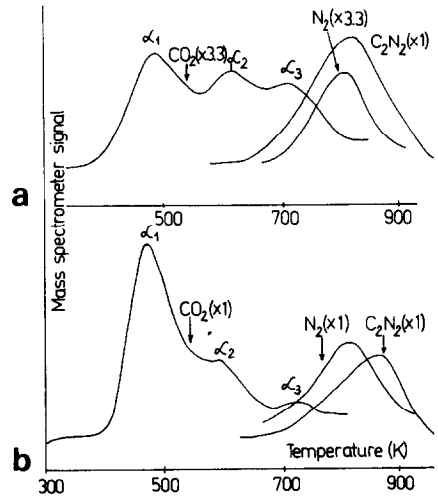

Fig. 6. Thermal desorption spectra following C_2N_2 adsorption at 300 K on a Cu(111) surface predosed with (a) 1.2 L O_2, (b) 60 L O_2. The C_2N_2 exposure was 90 L. The curves are uncorrected for detection sensitivities.

When the oxygen coverage was increased to $\theta \sim 0.17$, although the amount of adsorbed C_2N_2 decreased, relatively more CO_2 and N_2 were formed; the extent of C_2N_2 oxidation was about 45%. In this case more CO_2 desorbed in the first, and much less in the third stage. The peak temperatures of the first two stages were shifted to somewhat lower temperatures. The peak temperature of desorption of N_2 (T_{max}) was again 810 K. Unreacted C_2N_2 desorbed at a higher temperature ($T_{max} \sim 860$ K). Some characteristic TD curves are shown in fig. 6. Thermal desorption data are listed in table 1.

3.3. Electron energy loss studies

In agreement with previous studies [2,14,15], the characteristic loss energies of a Cu(111) surface appeared at 2.7, 4.8, 7.1, 18.0 and 26 eV. These losses did not vary with the primary electron energy.

The introduction of C_2N_2 onto a clean Cu(111) surface at 300 K produced new intense losses at 12.5 and 10.4 eV (fig. 7). The intensities of these peaks increased up to an exposure of about 12 L C_2N_2. At the same time the intensity of the peak at 18.0 eV decreased. The losses at 12.5 and 10.4 eV disappeared when the sample was heated above 860 K (fig. 7).

Admission of oxygen onto the surface (60 L, at 10^{-8} Torr) enhanced the intensities of the elastic peak and the 2.7 eV peak, and markedly reduced that of the peak at 18.0 eV. The peak at 7.1 eV was shifted to 6.5 eV. At 9.3 eV a new weak loss appeared (fig. 8).

Admission of C_2N_2 onto a Cu(111) surface predosed with only 1.2 L O_2 at 300 K, produced a loss at 10.4 eV and shoulders at 12.5 and 13.5 eV. As the C_2N_2

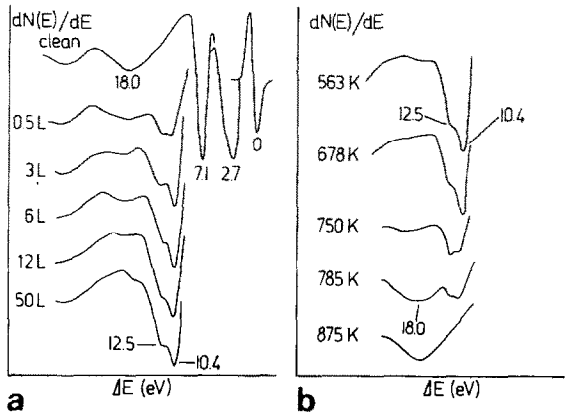

Fig. 7. Electron energy loss spectra of Cu(111) surface: (a) the effect of C_2N_2 exposure; (b) after heating the sample exposed to 90 L C_2N_2 to different temperatures (E_p = 70 eV; I_b = 0.2 μA).

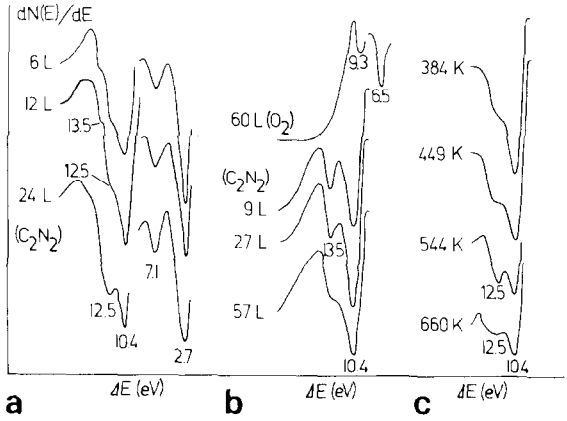

Fig. 8. Electron energy loss spectra of Cu(111) surface covered with oxygen as a function of C_2N_2 exposure: (a) 1.2 L O_2 ($\theta \approx 0.02$), (b) 60 L O_2 ($\theta \sim 0.17$). (c) After heating, the oxygen dosed sample ($\theta \sim 0.17$) exposed to 90 L C_2N_2 to different temperatures (E_p = 70 eV; I_b = 0.2 μA).

exposure increased, the 13.5 eV shoulder was hardly observable (fig. 8a). The appearance of the new loss or shoulder at 13.5 eV points to the formation of a new surface species in the interaction of adsorbed O and C_2N_2. The formation of this species became dominant when the C_2N_2 (9–27 L) was admitted onto the sample predosed with 60 L O_2 ($\theta \sim 0.17$). In this case intense losses appeared at 13.5 and 10.4 eV (fig. 8b). At higher C_2N_2 exposure a broad shoulder developed at 12–13 eV.

On heating of this sample to different temperatures, a decrease in the intensities of the new losses occurred above 400 K (fig. 8c). The loss at 12.5 eV was then well resolved. This disappeared together with the 10.4 eV loss above 860 K.

4. Discussion

4.1. Clean surface

The adsorption of C_2N_2 produced no ordered LEED pattern on a Cu(111) surface. The adsorption of C_2N_2 was also disordered on low index Pt surfaces [3,5] and on the stepped Pt surface at 300 K [9]. At saturation, the surface coverage $\theta \approx 0.2$ was reached. For the initial sticking probability we obtained a value of 0.1.

Admission of C_2N_2 onto a clean Cu(111) surface at 300 K produced losses at

12.5 and 10.4 eV in the electron energy loss spectra. It is to be mentioned that the adsorption of C_2N_2 on a Pt(100) surface produced loss features at 11 and 14 eV [8]. In this case, the electron energy loss measurements were performed with LEED optics as retarding field analyzer. The 14 eV loss was associated with π–π^* transitions from the states observed in the UPS at 6 eV below the Fermi level. The 11 eV loss was assumed to arise by electron promotion from the adsorbate related level 3 eV below the Fermi level to the same excited π^* states [8].

In the interpretation of the adsorption and desorption data, it is helpful to compare the behaviour of C_2N_2 on a Cu(111) surface with that observed previously on other surfaces. The characteristic values for the thermal desorption of C_2N_2 from different surfaces are listed in table 1.

TDS measurements indicate that C_2N_2 adsorbs in one stage on a Cu(111) surface at 300 K. The adsorbed phase is very stable; desorption began only above 700 K (T_{max} = 815–870 K). C_2N_2 also adsorbs in one stage on Ag(110) face [5]. In this latter case, however, C_2N_2 desorbed at very low temperature, above 323 K ($T_{max} \approx$ 430 K). This low temperature stage was similarly found on Pt(110) and Pt(100) surfaces and was unanimously attributed to the desorption of the non-dissociatively adsorbed C_2N_2 [3–6]. Apart from the very slight desorption observed around 450 K after high C_2N_2 exposure, there is no convincing evidence for the existence of this weakly bonded, non-dissociatively adsorbed C_2N_2 on the Cu(111) surface after adsorption at 300 K.

The temperature of desorption of C_2N_2 from Cu(111) approximates to that measured for the β stages on Pt(110) and Pt(100) surfaces, with the difference that no splitting of the high temperature peak was observed. The desorption temperature decreases with the increase of the coverage, indicating that the desorption follows second-order kinetics.

A reasonable proposal from these results is that C_2N_2 adsorbs dissociatively on the Cu(111) surface. The CN radical can not desorb as such, and its pairing is required for desorption, which occurs only at elevated temperatures. The temperature of desorption of C_2N_2 formed in the decomposition of NCO species adsorbed on the Cu(111) surface [1,2] agrees with that found in the present study. This may support the above conclusion, as the decomposition of NCO should lead first to the CN radical, which can be desorbed only after a recombination reaction.

As an alternative model it could be assumed that, due to an attractive lateral interaction between the C_2N_2 molecules in the adsorbed layer, a polymeric paracyanogen like structure is formed, similarly as was assumed by Netzer [4] in the case of Pt(100) surface. In order to decide whether this C_2N_2 structure exists on copper surfaces, too, UPS measurements are planned.

4.2. Oxygen-dosed surface

The presence of adsorbed oxygen exerted no promoting effect on the adsorption of C_2N_2 on a Cu surface; indeed, it rather decreased the uptake of C_2N_2. In this

respect it seems important to refer to the recent results on the interaction of HCN with this surface [16]. Similarly to the adsorption of HNCO [2], no adsorption of HCN was observed on the clean Cu(111) surface at 300 K. Preadsorbed O_2, however, induced the dissociative adsorption of HCN. The desorption spectrum following HCN adsorption was identical with that observed for C_2N_2 adsorption. There was no evidence for CN radical desorption; CN desorbed in the form of C_2N_2 above 700 K, showing that the pairing of CN radicals occurred on the surface.

The different adsorption behaviours of C_2N_2 and HCN on a Cu surface can easily be understood if it is assumed that the CN radical forms a strong bond with Cu, which promotes the dissociation of C_2N_2. As the bonding between Cu and H is very weak (hydrogen desorbs from Cu surface above 300 K [17]), from an energetic point of view the dissociation of HCN on a Cu surface is much less favoured compared to that of C_2N_2. In the presence of chemisorbed oxygen, however, due to the formation of OH groups the dissociation of HCN is greatly enhanced.

Mass spectrometric analysis of the gas phase during the adsorption of C_2N_2 on a Cu surface predosed with oxygen showed that below 373 K no reaction producing gaseous products takes place between the chemisorbed oxygen and C_2N_2. However, a well-detectable reaction occurs in the adsorbed phase above 400 K, yielding CO_2 and N_2.

As CO_2 adsorbs very weakly on clean and oxygen dosed copper, even at 300 K [2,17] we may assume that CO_2 formed in the surface reaction desorbs immediately after its formation, and thus the CO_2 desorption temperature is characteristic of the onset of the surface reaction. The fact that CO_2 desorbs in three stages could be explained by the assumption that (from the point of view of reactivity) different kinds of adsorbed oxygen exist on the surface. The studies carried out so far on the nature of chemisorbed oxygen on Cu(111) surfaces, however, provide no evidence for this assumption.

Another explanation is that the chemisorbed CN groups are in different environments; the CN reacts more easily with the adjacent adsorbed O, but the migration of the reactants is required when the adjacent adsorbed oxygen has been consumed. In accordance with this, an increase in the amount of adsorbed oxygen greatly increases the extent of low temperature oxidation, at the expense of the high temperature reaction (fig. 6).

Before formulating a more detailed reaction scheme of the interaction of adsorbed oxygen with CN groups and that of the oxidation reaction, we must take into account three important observations:

(i) In agreement with previous works [2–6], no electron-induced desorption or dissociation effects on adsorbed C_2N_2 and oxygen were observed. However, when both species were present on the surface, the O signal became very sensitive to the beam. The sensitivity of O signal to the electron beam increased with the increase of C_2N_2 coverage. A smaller beam effect was observed on the C signal, too. As similar phenomena were registered after the adsorption of HNCO on a Cu(111) surface [2], we might assume that an interaction occurred between adsorbed O and

CN groups at 300 K, resulting in surface NCO species.

(ii) This assumption seems to be supported by the ELS measurements. The adsorption of C_2N_2 on copper predosed with oxygen led to new losses at 10.4 and 13.5 eV, which were also observed after the adsorption of HNCO on this surface [2]. Although the adsorption of CO on Cu surfaces also produced a loss at around 13.5 eV [14,15], the observed 13.5 eV loss in the present work can not be attributed to the formation of adsorbed CO. The adsorption of CO on a clean Cu(111) surface was observed *only at low temperature* (140 K) [14,15] and the CO could be pumped off even at around 190 K.

(iii) The CO_2 desorption temperatures observed in the present study agree very well with those found in the reaction of NCO groups with adsorbed oxygen.

Further support for the formation of NCO groups in the interaction of surface O and CN group comes from a recent i.r. study of the adsorption of HCN and C_2N_2 on silica-supported copper oxides [18]. In this case an intense absorption band due to surface isocyanate was easily detected.

Accordingly, we propose the occurrence of the following reaction sequence in the interaction of C_2N_2 with a Cu(111) surface predosed with O_2 at 300 K:

$$C_2N_2 + Cu + Cu + Cu{-}O \rightarrow Cu{-}CN + Cu{-}CN + Cu{-}O\,, \tag{1}$$

and

$$C_2N_2 + Cu + Cu{-}O \rightarrow Cu{-}CN + Cu{-}NCO\,, \tag{2}$$

or

$$Cu{-}CN + O{-}Cu \rightarrow Cu{-}NCO + Cu\,. \tag{3}$$

On heating of the adsorbed layer to higher temperatures (up to 400 K), the reaction

$$Cu{-}NCO + O{-}Cu = Cu{-}N + CO_{2(g)} + Cu \tag{4}$$

occurs, which involves first the reaction of adjacent molecules, and then the migration of CN and NCO species to the more distant oxygen. Above 700 K, the recombination of adsorbed N atoms and the desorption of N_2 begins

$$Cu{-}N + N{-}Cu = 2\,Cu + N_2\,, \tag{5}$$

and also the pairing of unreacted CN radicals and their desorption in the form of C_2N_2

$$Cu{-}CN + NC{-}Cu = 2\,Cu + C_2N_2\,. \tag{6}$$

Although we cannot say anything definite from this study as regards the bonding mode of CN group to the Cu, in analogy to the Pt [6] and Ni [10] surfaces we may assume that it is multiply bonded to the Cu via both C and N atoms. This kind of bonding may promote the formation of –NCO species in the surface interaction between adsorbed CN and O.

The C_2N_2 desorption temperature was practically the same as in the case of the

clean surface. This is not surprising if we take into account that the bulk of the adsorbed oxygen had reacted before the desorption of the remaining C_2N_2.

We should also mention that the N_2 desorption temperature agreed very well with that observed for the desorption of N_2 (at the same coverage) formed in the oxidative decomposition of NCO species [2], and for the desorption of N_2 after adsorption of activated nitrogen [19] on Cu(111) surfaces.

References

[1] F. Solymosi and J. Kiss, in: Proc. IVC-8, ICSS-4, ECOSS-3, Cannes, 1980, Vol. I, p. 213.
[2] F. Solymosi and J. Kiss, Surface Sci. 104 (1981) 181.
[3] F.P. Netzer, Surface Sci. 52 (1975) 709.
[4] F.P. Netzer, Surface Sci. 61 (1976) 343.
[5] M.E. Bridge, R.A. Marbrow and R.M. Lambert, Surface Sci. 57 (1976) 415.
[6] M.E. Bridge and R.M. Lambert, Surface Sci. 63 (1977) 315.
[7] H. Conrad, J. Küppers, F. Nitschke and F.P. Netzer, Chem. Phys. Letters 46 (1977) 571.
[8] R.A. Wille, F.P. Netzer and J.A.D. Matthew, Surface Sci. 68 (1977) 259.
[9] F.P. Netzer and R.A. Wille, Surface Sci. 74 (1978) 547.
[10] J.C. Hemminger, E.L. Muetterties and G.A. Somorjai, J. Am. Chem. Soc. 101 (1979) 62.
[11] N.D. Spencer and R.M. Lambert, in: Proc. IVC-8, ICSS-4, ECOSS-3, Cannes, 1980, Vol. I, p. 395;
N.D. Spencer and R.M. Lambert, Surface Sci. 104 (1981) 63.
[12] M.E. Bridge and R.M. Lambert, J. Catalysis 46 (1977) 143.
[13] F.H.P.M. Habraken and G.A. Bootsma, Surface Sci. 83 (1979) 45.
[14] I. Kessler and F. Thieme, Surface Sci. 63 (1977) 405.
[15] H. Papp, Surface Sci. 63 (1977) 182.
[16] F. Solymosi and A. Berkó, to be published.
[17] J.E. Wachs and R.J. Madix, J. Catalysis 53 (1978) 208.
[18] F.S. Stone and T.H. Williams, presented at 7th Intern. Congr. on Catalysis, Tokyo, 1980.
[19] J. Kiss, A. Berkó and F. Solymosi, in: Proc. IVC-8, ICSS-4, ECOSS-3, Cannes, 1980, Vol. I, p. 521.